Summary of Models

1. Models

1.1. Full Firing Rate Model

Full model was used for the study in Chaos paper. The model consists of excitatory population with fast (AMPA-type) and slow (NMDA-type) excitatory synapses, fast (GABA_A,fast-type) and slow(GABA_A,slow-type) inhibitory populations, and a pool population.

$$\tau_e \cdot se_i = -se_i + f\left(gee\left(p\,se_i + (1-p)\sum se_k\right) + gne\left(p\,sn_i + (1-p)\sum sn_k\right) - gie\,si_{fast} - gse\,si_{slow} - \theta_e + \sigma_e + stim_e\right)$$

$$\tau_i \cdot si_{fast} = -si_{fast} + f\left(gei\sum se_i + gni\sum sn_i - gii\,si_{fast} - gse\,si_{slow} - \theta_i + \sigma_i + stim_i\right)$$

$$\tau_s \cdot si_{slow} = -si_{slow} + f\left(ges\sum se_i + gns\sum sn_i - \theta_s + \sigma_s\right)$$

$$\tau_n \cdot sn_i = -sn_i + a_n\,se_i\left(1-sn_i\right)$$

where τ_e, τ_i, τ_s , and τ_n are time constants for excitatory, fast inhibitory, slow inhibitory, and slow excitatory synapses, respectively. We used nonlinearity function $f(x) = a\sqrt{\frac{x-c}{1-e^{-b(x-c)}}}$. The full model also has a local delay between each population and a global time delay between each network.

1.2. Reduced Firing Rate Model

We started the same model as used for the Chaos paper to extend the model in terms of the number of populations as well as different network architectures. But, the model seemed to be too complicated to work with for a few reasons. First, the model included the slow inhibition which seemed to strongly modulate the overall dynamics of the system and it made the analysis too complicated. So, we dropped this component later. Second, the model had time delays for both local and global interactions. This made it difficult to use AUTO or bifurcation analysis. So, we removed any time delay afterwards. Third, the model had the pool population which also seemed to modulate the system dynamics as the coupling strength with other populations gets stronger although the pool itself is never excitable by itself. But, the pool was very weakly coupled with all the other populations, anyway. So, we also removed the pool. All these additional components made the dimension of the system way too high to effectively analyze the system dynamics. Thus, we came up with reduced model composed only of AMPA-type fast excitatory synapse, NMDA-type slow excitatory synapse, and GABA_A-type fast inhibitory synapse. We call this model a "reduced model".

$$\tau_e \cdot se_i = -se_i + f\left(gee\left(p\,se_i + (1-p)\sum se_k\right) + gne\left(p\,sn_i + (1-p)\sum sn_k\right) - gie\,si_{fast} - \theta_e + \sigma_e + stim_e\right)$$

$$\tau_i \cdot si_{fast} = -si_{fast} + f\left(gei\sum se_i + gni\sum sn_i - gii\,si_{fast} - \theta_i + \sigma_i + stim_i\right)$$

$$\tau_n \cdot sn_i = -sn_i + a_n se_i(1 - sn_i)$$

Now, the reduced model shows attractors shown in the left figure when single input is given, and in the right figure when the 2-parameter bifurcation analysis is used.

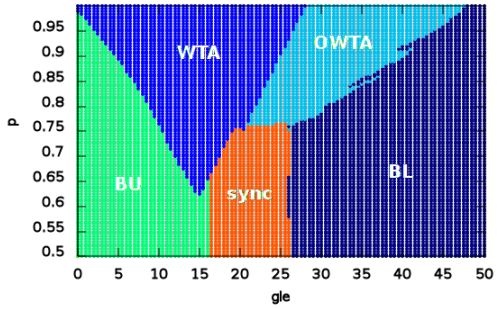

Figure 1.A

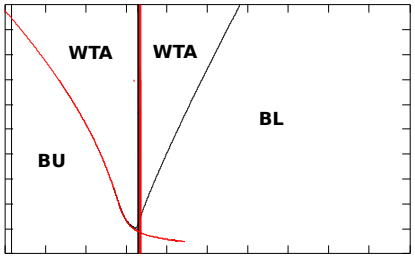

Figure 1.B

This input-output map for two excitatory population model nicely matches the two-parameter plot obtained by XPPAUTO. Having such a response map, we wanted to examine how transitions from one attractor to another can be achieved and what input protocols are required for each transitions.
We also extended the model to include more excitatory populations. Figure 4.A shows p-vs-gie map for 5 population model when multiple inputs (4 inputs) are applied to the system when it is in baseline.

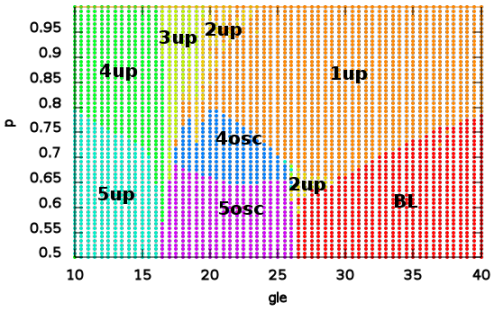

Figure 4.A

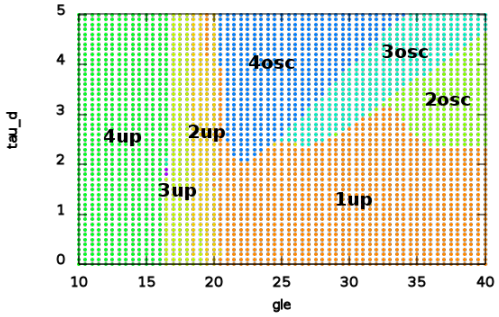

Figure 4.B

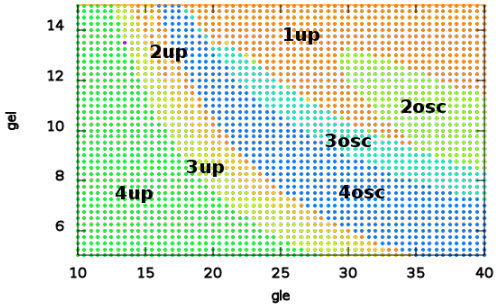

Figure 4.C (p=0.9)

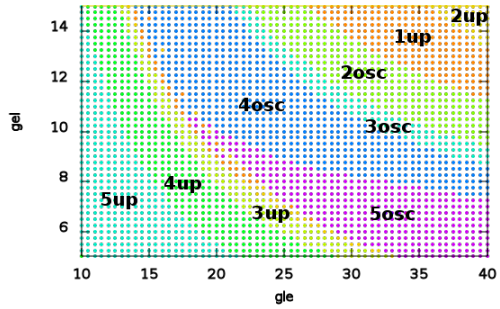

Figure 4.D (p=0.8)

When the local time delay is turned back on, various states can be obtained as the time delay and gie

change revealing similar types of states as in Figure 4.A. In both figures, multiple WTA and multiple synchronous OWTA states can be seen including possible seizure states such as "5up" and "5osc" for multiple inputs. Figure 4.C and Figure 4.D compare gei-vs-gie map for different p values, $p=0.9$ and $p=0.8$, respectively. Such gei-vs-gie map clearly demonstrates that the level of inhibition determined by E-to-I connection strength and I-to-E connection strength doesn't necessarily symmetric in their effects on the resonpose of the system to multiple inputs. Also, it should be noted that as p gets smaller seizure states such as "5up" or "5osc" emerge.

1.3. Boundary Value Problem For Reduced Firing Rate Model

After a few preliminary tests by solving the IVP, we were interested in the different dynamics between WTA and OWTA in terms of minimum amplitudes to activate the system, switch the memory states, and terminate existing memory state. To get numerically more exact solutions to this problem, we formulate the problem in BVP with particular initial conditions.

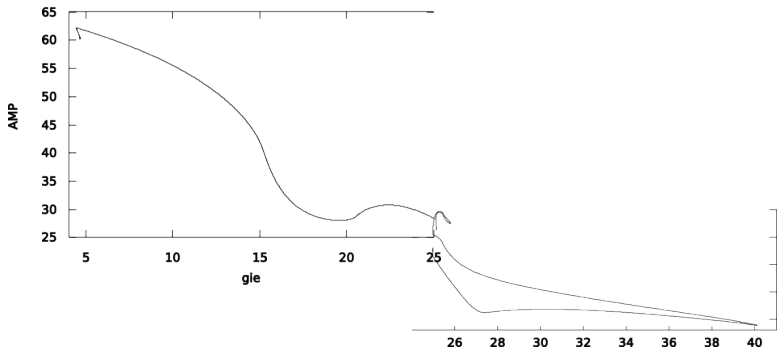

Figure 2.A

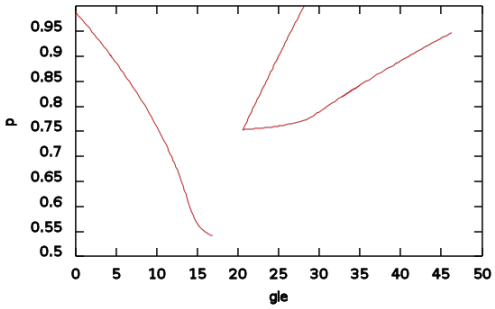

Figure 2.B

The left figure shows the minimum amplitude to make a switch from one memory state to another memory state as gie increases from 5 to 40 where the transition between WTA and OWTA happens at $gie \simeq 25$. The right figure shows p-vs-gie revealing similar domains show in Figure 1.B.
By solving BVP for a few cases, we observed that OWTA state requires smaller amplitude to make a switch to another memory state. But, there were also other factors, for example, timing of input to the system when it is already in OWTA state, that limited usefullness of BVP formulation.
Having solved BVP for limited issues, we wanted to test some observations with "reduced" population model using spiking neuron model.

1.4. Spking Neuron Model

The spiking neuron model is based on theta neurons with same synapses for the reduced firing rate model.

$$\tau_e \cdot ve_{l,i} = (1-\cos(ve_{l,i})) + (1+\cos(ve_{l,i})) \cdot \left(gee \left(p \sum_k w \cdot se_{l,k} + (1-p) \sum_k w \cdot se_{m,k} \right) \right.$$
$$\left. + gne \left(p \sum_k w \cdot sn_{l,k} + (1-p) \sum_k w \cdot sn_{m,k} \right) - gie \sum_k w \cdot si_k - \theta_e + \sigma_e + stim_e \right)$$

$$\tau_e \cdot vi_i = (1-\cos(vi_i)) + (1+\cos(vi_i)) \cdot \left(gei \sum_l \sum_k w \cdot se_{l,k} + \sum_l \sum_k w \cdot sn_{m,k} - gii \sum_k si_k - \theta_i + \sigma_i + stim_i \right)$$

where $ve_{l,i}$ and vi_i are theta neurons of excitatory and inhibitory populations. Here, l and m denote population numbers, and i and j denote neuron numbers.
We first examined two population model with 100 neurons in each popution and applied same set of parameters used for the reduced firing rate model.

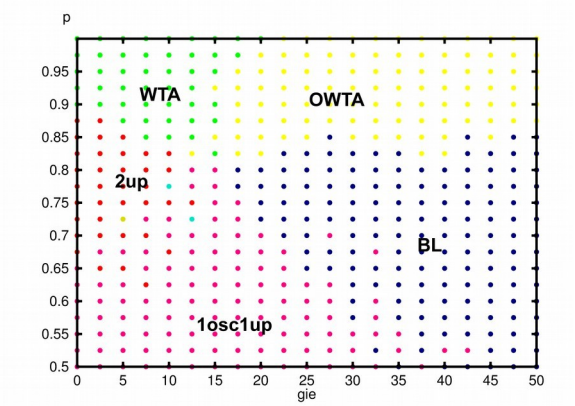

Figure 3.A

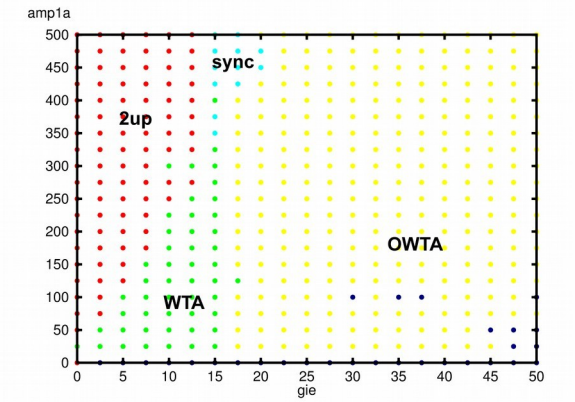

Figure 3.B

Figure 3.A shows p-vs-gie relation when a single input is given to the system. Dependig on p and gie values, there are various states including a mixed state with one population in oscillatory state and the other in persistent "up" state. Also, the boundaries between each state change as the amplitude of input changes (not shown). Figure 3.B shows amp-vs-gie relation for fixed p ($p=0.9$) revealing large OWTA domain.

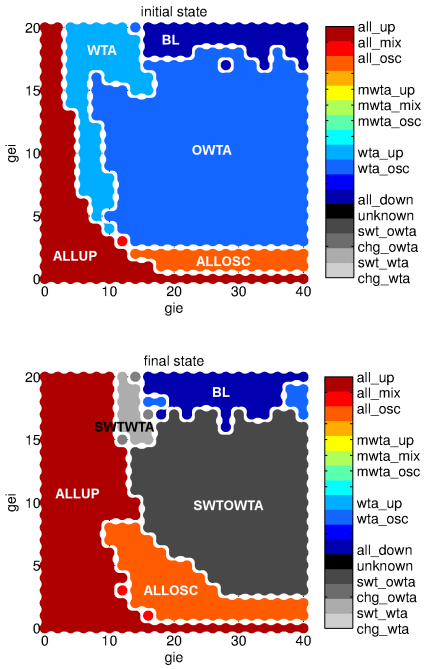

Figure 4.A (p=0.1)

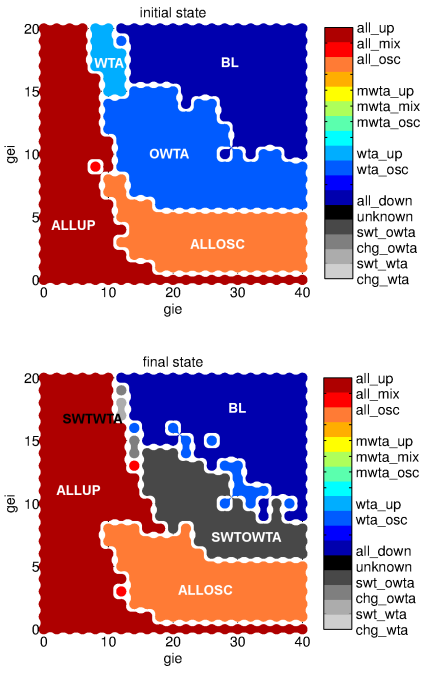

Figure 4.B (p=0.2)

Figure 4 shows how the system changes (or maintains) its memory state. The upper panel shows the first state of the system after the first input is given to population 1 when it is initially in the baseline state, and the lower panel shows the final state of the system after the second input is given to population 2. Figure 4.A (left) is when p is 0.1 and Figure 4.B is when p is 0.2. **Note that p is now the level of crosstalk, whereas p was previously the level of sprouting.** By comparing the initial states in Figure 4.A and B, it is clear that both WTA and OWTA regions diminish and the seizure states ("all up" or "all osc") expand and intrude into WTA and OWTA regions as p decreases. Also, comparison of initial states and the final states shows that WTA state is very hard to switch compared to OWTA state, i.e., majority of WTA regions in the upper panels become a seizure state ("all up") whereas majority of OWTA regions turn into the other memory state (population 2) except for smaller gie or gei values. This observation is consistent with the previous result with the reduced firing rate model.

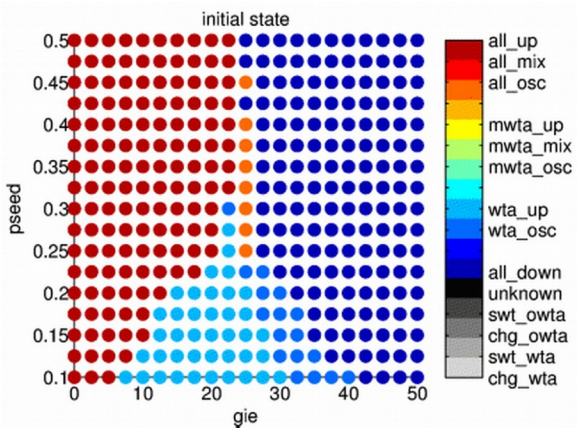

Figure 5.A

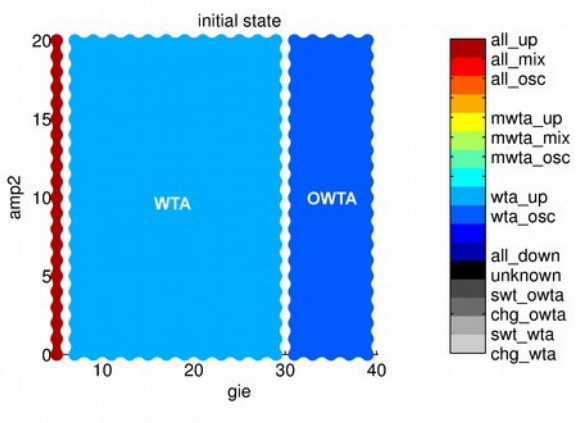

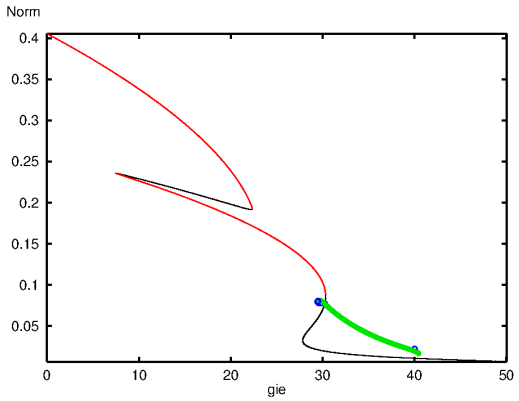

Figure 5.B

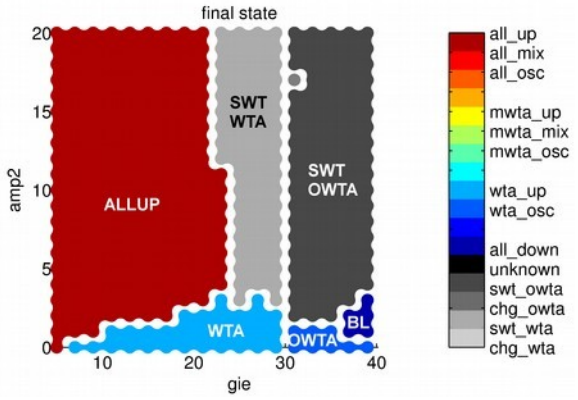

Figure 5.C

Figure 5.A shows single input response of the system in p-gie space. This matches the p-vs-gie map of the reduced firing rate model for two population (when p is flipped upside down as the definition of p has been changed). Figure 5.B is the bifurcation diagram of the reduced firing rate model with equivalent parameters. There is a tri-stable region between $gie=8$ and $gie=22$ (baseline is always stable) followed by bistable regions with stable fixed points ($22 \le gie \le 30$) and stable periodic solutions($30 \le gie \le 40$) as gie increases. Figure 5.C shows how the minimum amplitude to switch the memory state changes as gie changes. Increasing gie makes the system transition from "all up" state to WTA and OWTA state when the first input is given to population 1 which in initially in the baseline. When the second input is given to population 2 with various amplitude, large area of WTA state becoms "all up" state ($gie \simeq 23$) whereas most of the OWTA area switches ("swt owta") leaving

very small area in baseline state or not affected at all. In addition, the minimum amplitude to successfully switch the memory state from one to another steeply increases as gie gets down to about 23 passed through the boundary between OWTA and WTA. But, it doesn't exactly occur at the boundary. With two population model, it is not clear whether or not "all up" and "all osc" are really seizure states due to the fact that there are only two populations, nor we can talk about capacity. Thus, we extend the system size to 10 populations.

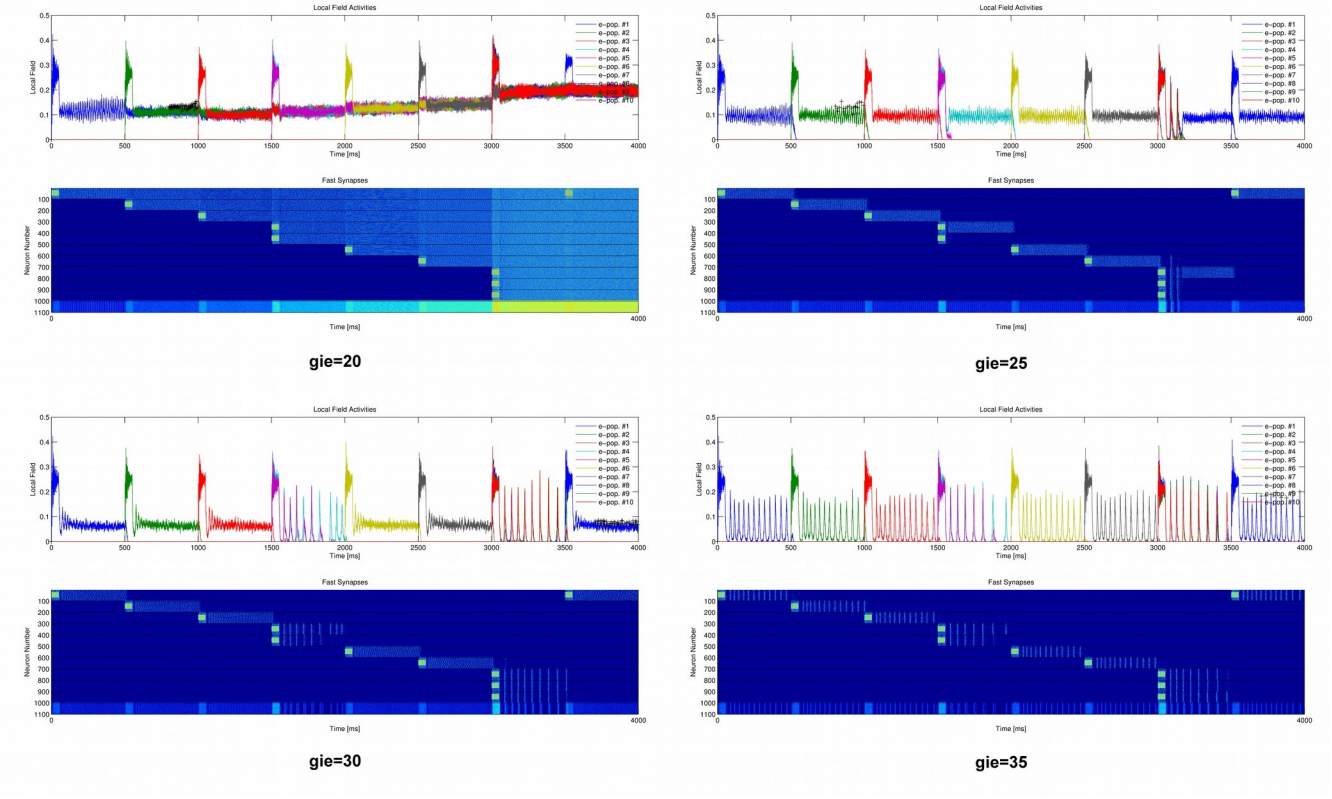

Figure 6.

Figure 6 shows how the system responses to the sequential inputs including single, double, and tripple inputs for various gie. When gie is 20, the system has capacity of 10 and each population is in asynchrous up state when excited. Also, it can take double input or triple input simultaneously. As gie increases to 25, the system looses its capacity and can only maintain one memory state in asynchronous up state. Also, when multiple input is given, only one population retains its memory state after the competition. As gie further increases to 30, multiple input causes the system to synchronously oscillate in beta rhythm, and seems to have finite capacity of two or three in oscillatory mode. When gie becomes 35, all the memory states are oscillatory and the oscillation frequency of single memory state is higher than that of multiple memory states (1500-2000ms and 3000-3500ms)

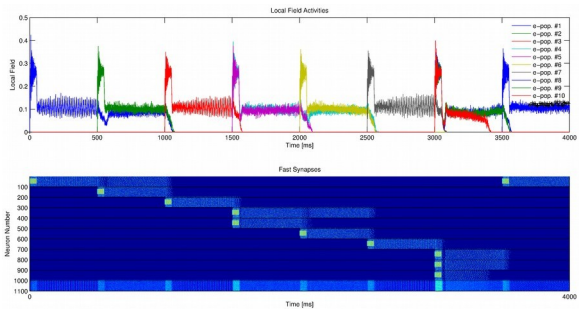

Figure 7.A (gie=22)

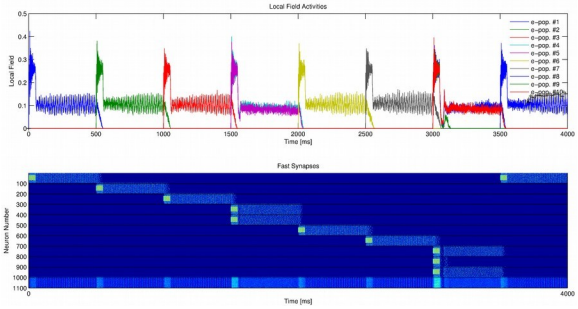

Figure 7.B (gie=23)

The system, however, does not necessarily have to be in oscillatory mode to have finite capacity over one. As Figure 7 shows, the system can have finite capacity of two in asynchronous up state although only multiple input can activate multiple memory state in case of gie=23.
After some preliminary tests for 10 population model, we wanted to make the two model, i.e., the reduced firing rate model and the spiking neuron model, consistent with each other. Hence, we introduce the membrane time constant τ_m in front of the square root of the nonlinearity so that the mean field firing rate f(I) becomes

$$f(I)=\frac{1}{\pi\tau_m}\sqrt{\frac{x-c}{1-e^{-b(x-c)}}}$$

where b and c are tuned to yield proper dynamics. But, with large membrane time constant ($\tau_m \simeq 10$) it is hard to get multiple OWTA mode. So we introduce adaptation to the reduced model and the system of equations becomes

$$\tau_e \cdot se_i = -se_i + f\left(gee\left(p\,se_i + (1-p)\sum se_k\right) + gne\left(p\,sn_i + (1-p)\sum sn_k\right) - gie\,si_{fast} - gz\,ze_i - \theta_e + \sigma_e + stim_e\right)$$

$$\tau_n \cdot sn_i = -sn_i + a_n\,se_i\left(1-sn_i\right)$$

$$\tau_z \cdot ze_i = -ze_i + a_z\,se_i$$

When the parameters for the reduced firing rate model is properly tuned, we can get desired dynamics of working memory such as different single memory state, i.e., persistent (asynchronous) and oscillatory(synchronous) state, switchability of memory state by external input, finite capacity in both persistent and oscillatory modes, and different oscillation frequency, etc.

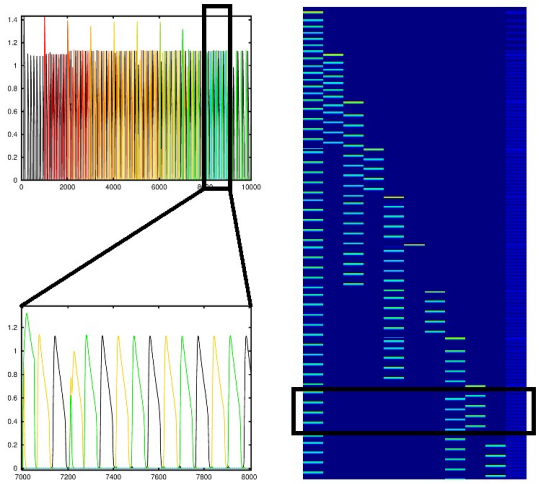

Figure 8.A Figure 8.B

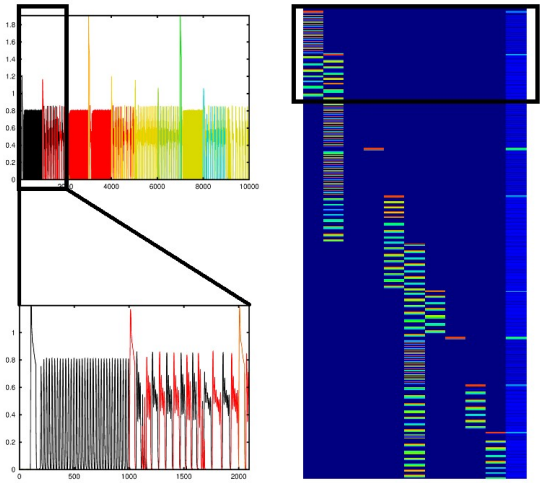

Figure 9.A Figure 9.B

Figure 8 shows a case of multiple OWTA with oscillation frequency dictated by adaptation. When there is a multiple oscillatory memory state, all populations oscillate out of phase relative to another. Also, the larger the memory state is, the slower the oscillation frequency is. It is noted that a new input sometimes fails to activate memory state (6th input in Figure 8.B). Figure 9 is another example of multiple OWTA but with smaller capacity of only two. In this case, it should be noted that there is a gamma oscillation when only one memory state is active and theta oscillation when two memory states

are active. But, as the lower panel of Figure 9.A shows, a faster oscillation at gamma frequency is embedded in theta oscillation even in multiple OWTA. Also, again sometimes a new input fails to activate a new memory state as 3rd, 4th, and 8th inputs in Figure 9.B show.
Depending on the combination of adaptation level and inhibition level, the duration of embedding of gamma oscillation in theta oscillation (or gamma-theta cross frequency coupling) can be longer as Figure 10 demonstrates.

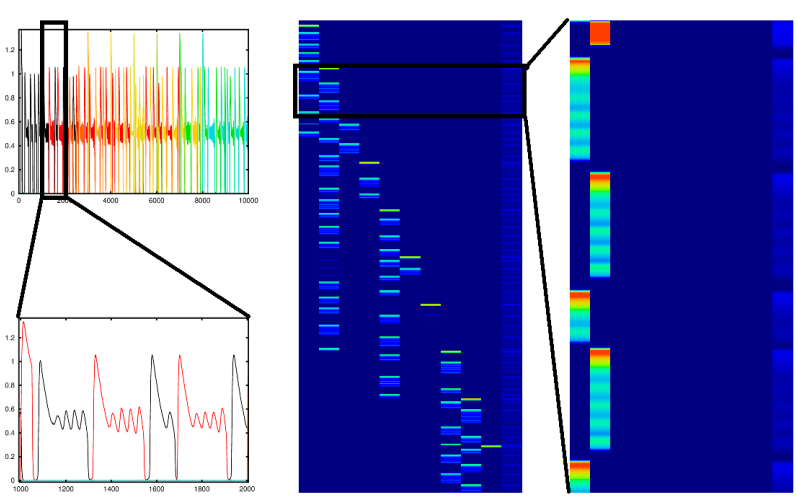

Figure 10

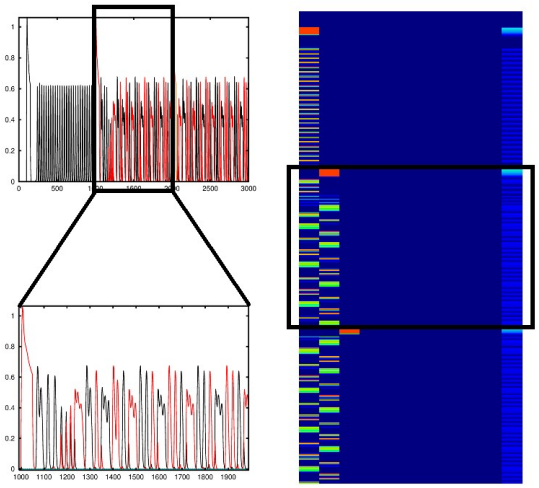

Figure 11

Figure 10 shows the gamma-theta cross frequency coupling, and the frequency of the faster oscillation is dictated by the time constant of inhibition (τ_i) whereas the frequency of the slower oscillation is dictated by the time constant of adaptation (τ_z). In Figure 11, two populations alternate switching memory state with each other, and a series of singlet, doublet, and embedded gamma oscillation can be seen. Based on the same set of parameters used above, the spiking neuron model is used to examine the behavior of the 10 population model.

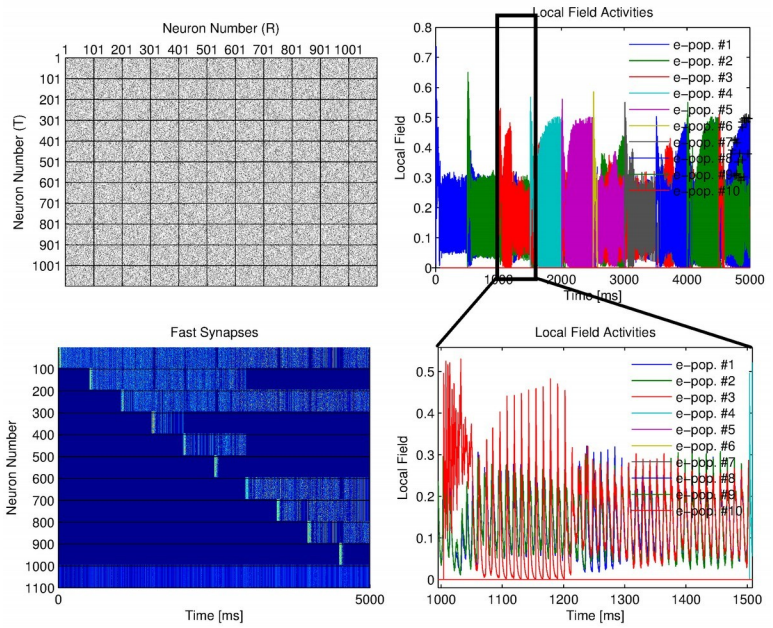

Figure 12

When the same set of parameters are applied to the spiking neuron model with uniform connection density of 0.2, multiple OWTA dynamics can be obtained as shown in Figure 12. The system has a finite capacity of 4 or 5, and the oscillation frequency is about 90-100Hz in synchronous manner. Depending on the inhibition level (gie) different capacity and oscillation frequency can be obtained. For most of the simulations both for the firing rate model and the spiking neuron model shown above, p was fixed at 0.1~0.15.

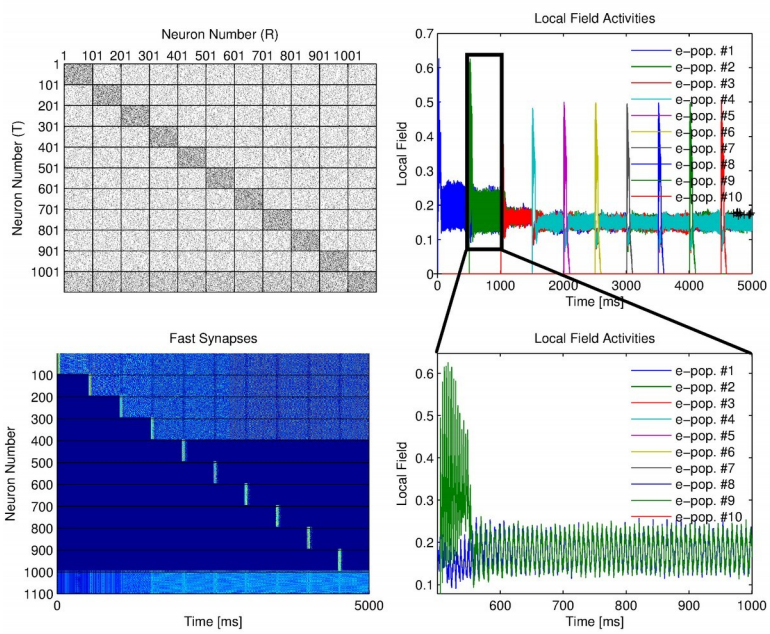

Figure 13

When nonuniform connection density (inner population=0.3, interpopulation=0.1, I-to-E=0.2) is used with the same set of parameters, the system has a finite capacity of 4. Interestingly, when the number of memory is either 1 or 2, all the neurons synchronously oscillate at very high frequecy (~130Hz), whereas all the neurons asynchronously oscillate for the memory state of 3 or 4. Also, once the system gets into asynchronous mode, it resists to any further input with the same amplitude, which is conincident with the previous observation for two populationmodel where switching is very difficult for asynchronous WTA mode.